

Targeting Coenzyme Q10 synthesis overcomes bortezomib resistance in multiple myeloma

Esther A. Zaal^{1,2}, Harm-Jan de Grooth^{3*}, Inge Oudaert^{4*}, Pieter Langerhorst¹, Sophie Levantovsky², Gijs J.J. van Slobbe², Jeroen W.A. Jansen², Eline Menu⁴, Wei Wu^{1,5}, Celia R. Berkers^{1,2#}

Supplementary Information

¹ Biomolecular Mass Spectrometry and Proteomics, Bijvoet Centre for Biomolecular Research and Utrecht Institute of Pharmaceutical Sciences, Utrecht University, Utrecht, The Netherlands

² Division of Cell Biology, Cancer & Metabolism, Department of Biomolecular Health Sciences, Faculty of Veterinary Medicine, Utrecht University, Utrecht, The Netherlands

³ Department of Intensive Care & Department of Anesthesiology, Amsterdam University Medical Centers, Location VUmc, Amsterdam, The Netherlands.

⁴ Department of Hematology and Immunology, Myeloma Center Brussels, Vrije Universiteit Brussel, Brussels, Belgium.

⁵ Netherlands Proteomics Centre, Utrecht, The Netherlands

Supplementary Methods

Liquid chromatography – Mass Spectrometry based Metabolomics

For all experiments, cells were resuspended in fresh medium 16-24 hours prior to the start of the experiment. At the start of all experiments, cells were counted and centrifuged for 5 minutes at 1400 rpm to remove the old medium. For metabolic screens, cells were resuspended in fresh RPMI medium at a density of 1×10^6 cells/ml. After 2 hours, samples were washed with PBS and harvested by centrifugation for 5 min at 1000g at 4°C. Metabolites were extracted by adding 100 – 200µl ice-cold MS lysis buffer (methanol/acetonitrile/uLCMS H₂O (2:2:1)) to the cell pellets. Samples were shaken for 10 minutes at 4°C, centrifuged at 14,000g for 15 minutes at 4°C and supernatants were collected for LC-MS analysis.

For ¹³C-tracer experiments, cells were resuspended in DMEM containing 2 mM [U-¹³C]D-Glutamine (Cambridge Isotopes) and 25 mM ¹²C-glucose or 2mM ¹²C-glutamine and 25 mM [U-¹³C]D-Glucose and harvested after 4 hours as described above. For glutamine starvation experiments, medium consisted of DMEM, supplemented with 25 mM [U-¹³C]D-Glucose and 10% dialyzed FBS in the presence or absence of 2 mM L-glutamine. Cells were resuspended at a density of 0.7×10^6 in triplicate wells and were harvested after 4 hours as described above. To measure extracellular metabolites, medium samples were obtained prior to harvesting cells at 8 or 24 hours. Metabolites were extracted by diluting 10µL medium in 1mL MS lysis buffer. For the effect of simvastatin on metabolism, cells were resuspended in fresh RPMI medium at 1×10^6 cells/ml in the presence or absence of 1 µM simvastatin and harvested after 24 hours as described above.

LC-MS analysis was performed on an Exactive mass spectrometer (Thermo Scientific) coupled to a Dionex Ultimate 3000 autosampler and pump (Thermo Scientific). The MS operated in polarity-switching mode with spray voltages of 4.5kV and -3.5kV. Metabolites were separated on a Sequant ZIC-pHILIC column (2.1 x 150mm, 5µm, Merck) with guard column (2.1 x 20mm, 5µm, Merck) using a linear gradient of acetonitrile and a buffer containing 20mM (NH₄)₂CO₃, 0.1% NH₄OH in ULC/MS grade water. Flow rate was set at 150 µL/min. Metabolites were identified based on exact mass within 5 ppm and further validated by concordance with retention times of standards. Metabolites were quantified using LCQuan software (Thermo Scientific). Peak intensities were normalized based on median peak intensity and isotope distributions were corrected for natural abundance. Peak areas of identified metabolites were in their respective linear range of detection.

Proteomics with membrane fractionation

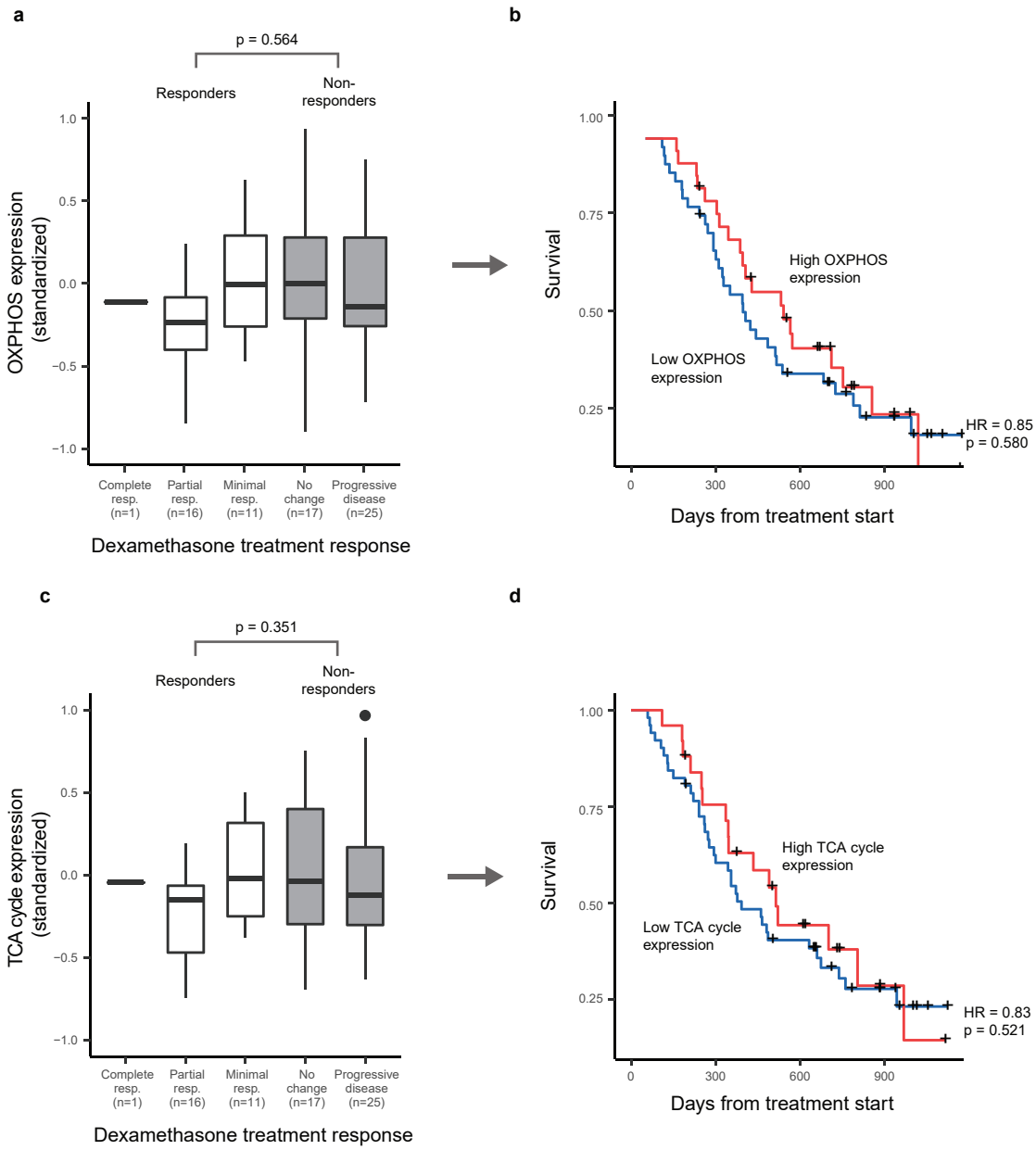
RPMI-8226 WT and BTZ-resistant cells were seeded in RPMI medium at a density of 1×10^6 cells/ml and incubated for 2 hours. Per treatment category, four biological replicates of 3×10^7 cells were washed with PBS and harvested for fractionation using a plasma membrane isolation kit (Abcam, ab65400). Cell pellets were gently lysed on ice using a dounce homogenizer in the presence of protease inhibitor (cOmplete mini EDTA-free, Roche) and phosphatase inhibitor (PhosSTOP, Roche). Differential centrifugation according to manufacturer's instructions yielded the cytosolic fraction, inner membrane and finally plasma membrane. Thirty micrograms of protein each from the cytosolic, inner membrane and plasma membrane fraction were reduced in 4mM Dithiothreitol, alkylated in 8mM iodoacetamide, and digested sequentially at 37°C with 1:75 Lys C (Wako) and 1:50 Trypsin (Sigma-Aldrich) for 4 and 12 hours respectively. Digested peptides were acidified to 0.1% formic acid (FA) and purified by strong cation exchange (SCX) STAGE tips. Eluted peptides were dried by vacuum and 2µg equivalent of peptides was analysed in each 3hr reverse phase separation on the UHPLC 1290 system (Agilent) coupled to an Orbitrap Q Exactive Plus mass spectrometer (Thermo Scientific). Proteomics data were acquired using an UHPLC 1290 system (Agilent) coupled to an Orbitrap Q Exactive Plus mass spectrometer (Thermo Scientific). Peptides were first trapped on a 2 cm x 100 µm Reprosil C18 pre-column (3 µm) and then separated on a 50 cm x 75 µm Poroshell EC-C18 analytical column (2.7 µm). Trapping was performed for 5 min in 0.1 M acetic acid (Solvent A) and elution with 80% ACN in 0.1M acetic acid (Solvent B) in gradients as follows: 10-36% solvent B in 155 min, 36-100% in 3min and finally 100% for 1min. Flow was passively split to 300 nl/min. MS data were obtained in data-dependent acquisition mode. Full scans were acquired in the m/z range of 375-1600 at the resolution of 35,000 (m/z 400) with AGC target 3E6. Top 15 most intense precursor ions were selected for HCD fragmentation performed at NCE 25% after accumulation to target value of 5E4. MS/MS acquisition was performed at a resolution of 17,500.

Raw files were processed using MaxQuant version 1.5.3.30 and searched against the human Swissprot database (version Jan 2016, 147933 entries) using Andromeda. Cysteine carbamidomethylation was set to fixed modification, while variable modifications of methionine oxidation and protein N-terminal acetylation, as well as up to 2 missed cleavages were allowed. False discovery rate (FDR) was restricted to 1% in both protein and peptide identification. Label-free quantification (LFQ) was performed with "match between runs" enabled.

Cholesterol and CoQ analysis by LC-MS

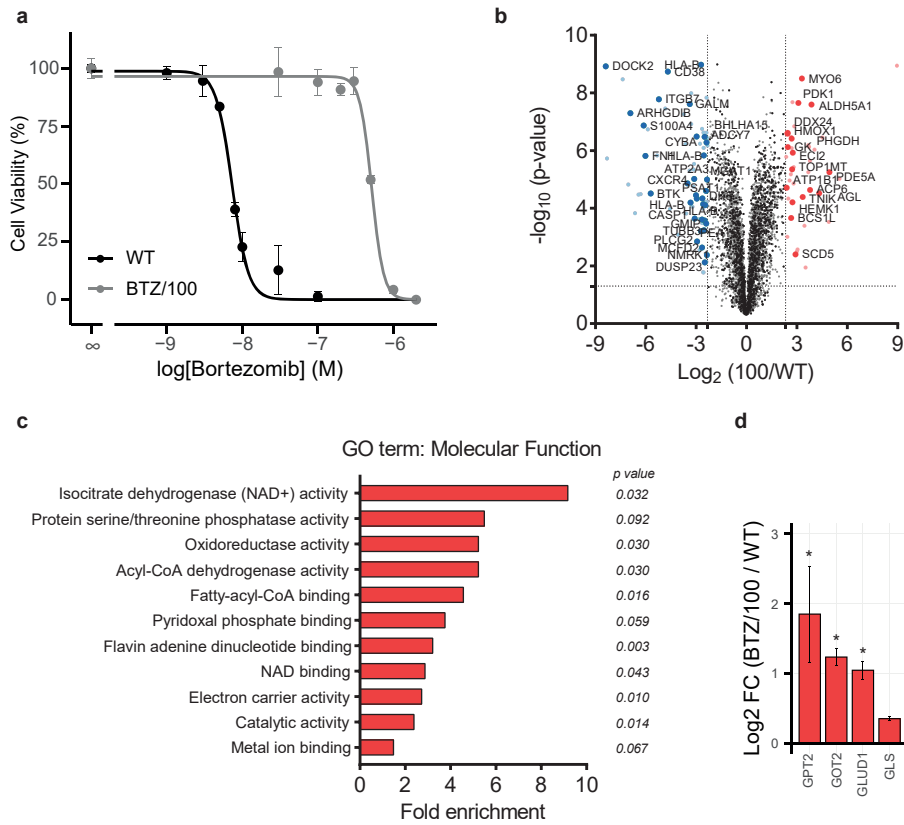
RPMI 8226 WT and BTZ/100 cells were resuspended in fresh RPMI medium at a density of 1×10^6 cells/ml in the presence or absence of $1 \mu\text{M}$ simvastatin. After 24 hours, samples were washed with PBS and harvested by centrifugation for 5 min at 1000g at 4°C . Cells were resuspended in 800 μL PBS and transferred to round bottom glass tube. Cholesterol and CoQ were extracted according to Bligh and Dyer [41]. LC-MS analysis was performed on an Q-Exactive HF mass spectrometer (Thermo Scientific) coupled to a Vanquish autosampler and pump (Thermo Scientific). 10 μL aliquots were injected directly onto a Kinetex/HALO C8-e column (2.6 μm , 150×3.00 mm; Phenomenex, Torrance, CA, USA). Gradient elution was performed from methanol/water (1/1; v/v) to methanol/isopropanol (4/1; v/v) in 2 minutes, followed by isocratic elution with the latter solvent for an additional 5.5 minutes. Flow rate was kept constant at 600 $\mu\text{L}/\text{min}$ and a 2.5 minute re-equilibration time was used between runs. Mass spectrometry of eluting lipids was performed using positive mode Atmospheric Pressure Chemical Ionization (APCI) on a Q-Exactive HF mass spectrometer (Thermo) in the range from 150–1100 Da. Cholesterol and CoQ were quantified using TraceFinder software (Thermo Scientific) and identified based on exact mass within 5 ppm and further validated by concordance with retention times of standards. Peak areas of identified metabolites were in their respective linear range of detection.

Supplemental Figure S1



Supplemental Figure S1: Expression of the OXPPOS and TCA cycle KEGG pathways was not associated with dexamethasone resistance or survival in multiple myeloma patients. Tumor cell gene expression data was available for 70 multiple myeloma patients before the start of dexamethasone therapy. After standardizing the population-wide expression of each gene to mean=0, SD=1, the mean expression of the KEGG oxidative phosphorylation pathway (132 genes, 110 measured) and the KEGG TCA cycle pathway (30 genes, 29 measured) was calculated for each patient. **a.** Expression of the OXPPOS pathway before the start of therapy was not associated with treatment response to dexamethasone. **b.** OXPPOS pathway expression was not associated with overall survival under dexamethasone therapy. **c.** Expression of the TCA cycle pathway before the start of therapy was not associated with treatment response to dexamethasone. **d.** TCA cycle pathway expression was not associated with overall survival under dexamethasone therapy. Expression by treatment response was compared using t-tests, survival was compared using a Cox Proportional Hazards model. Crosses indicate censoring of survival information.

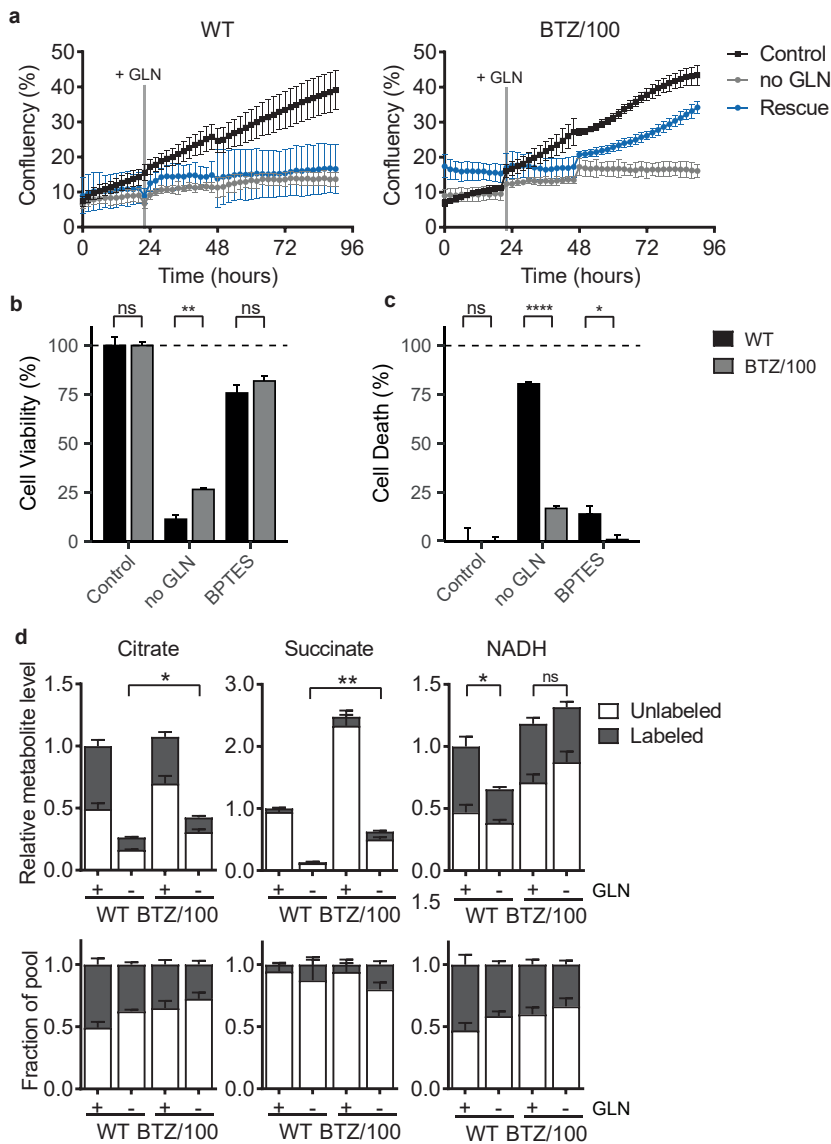
Supplemental Figure S2



Supplemental Figure S2: Analysis of metabolic enzymes associated with bortezomib resistance

a A representative graph of the response of RPMI-8226 wild type (WT) (black) and bortezomib-resistant (BTZ/100) (grey) cells after a 48-hour treatment with increasing concentrations of Bortezomib. Results represent % cell viability \pm SD compared to non-treated controls ($n=3$). **b** Graphical representation of quantitative proteomics data. Proteins are ranked in volcano plot according to their statistically p-value (y-axis) and relative abundance ratio between RPMI-8226 wild type (WT) and bortezomib resistant (BTZ/100) cells (x-axis). Coloured spots represent significantly upregulated (red) or downregulated (green) proteins in BTZ/100 cells with at least a 5-fold change. Significantly regulated metabolic enzymes are marked. **c** Gene Ontology (GO) enrichment analysis of upregulated metabolic enzymes in BTZ/100 cells (≥ 2 -fold, $p < 0.05$). **d** Bar graphs display the average log_2 fold change (FC) of metabolic enzymes involved in glutaminolysis. Enzymes that were significantly up- (red) or downregulated (blue) in RPMI-8226 bortezomib-resistant (BTZ/100) cells compared to wild type (WT) are marked with *.

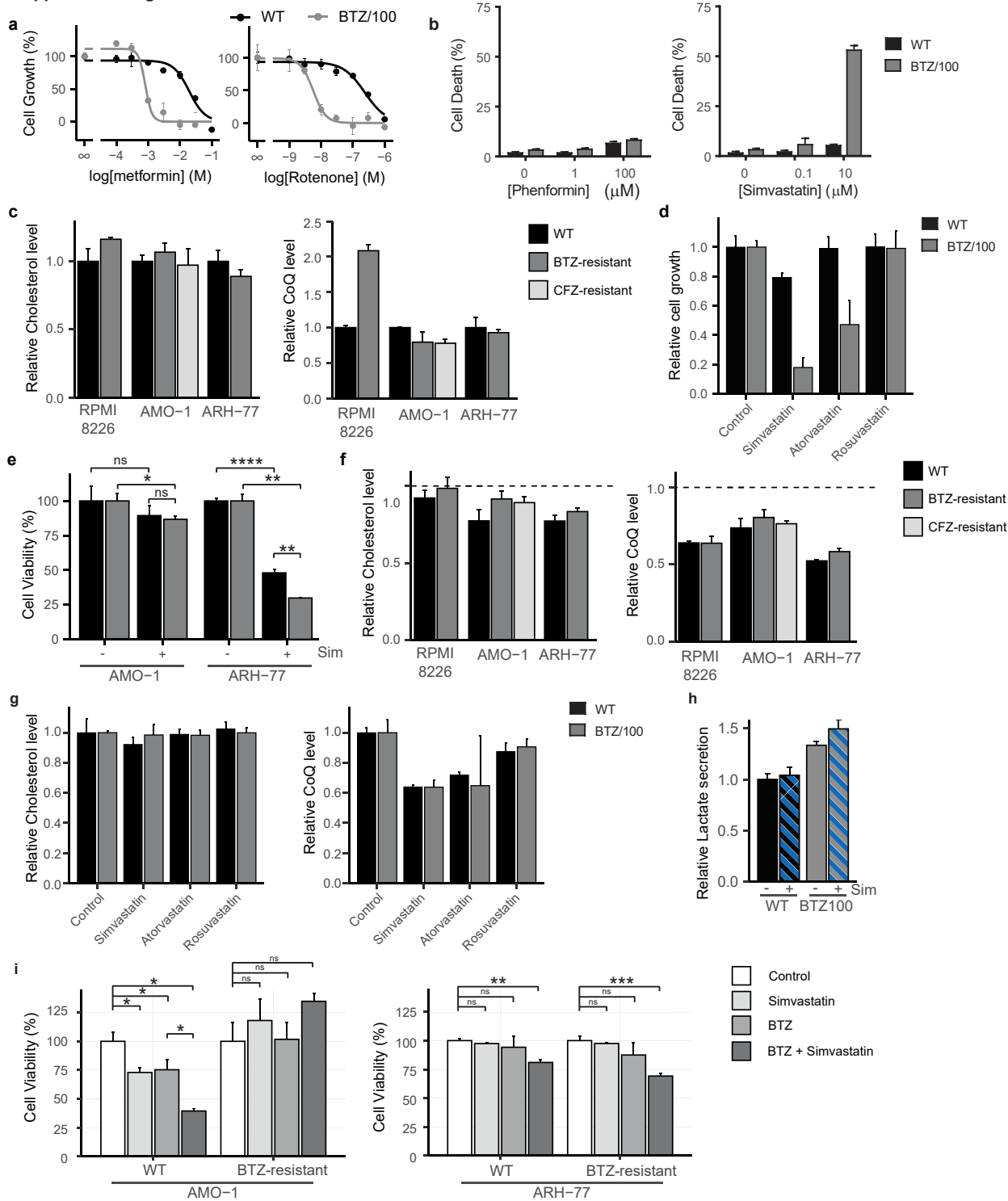
Supplemental Figure S3



Supplemental FigureS3: Bortezomib-resistant cells are less dependent on extracellular glutamine for survival

a Confluency of RPMI-8226 wild type (WT) (left panel) and bortezomib-resistant (BTZ/100) (right panel) cells followed over time in the presence (black) or absence (grey) of glutamine (GLN). Glutamine was added after 24 hours in cells that were starved for glutamine (blue). Results represent % of confluency (n=3). **b** Intracellular analysis of TCA cycle intermediates of RPMI-8226 wild-type (WT) and BTZ/100 cells. Cells were resuspended in DMEM containing 2 mM [U-¹³C]D-Glutamine. Intracellular metabolites were extracted after 8 hours and analyzed by LC-MS. Data are means ± SD (n=3) of unlabelled (white) and ¹³C-labelled (blue) metabolites as compared to WT (upper panel). Isotopic distributions are depicted in the lower panel.

Supplemental Figure S4



Supplemental FigureS4: Bortezomib-resistant cells are less dependent on extracellular glutamine for survival

a Growth rate of RPMI-8226 wild type (WT) (black) and bortezomib-resistant (BTZ/100) (grey) cells after a 48-hour treatment with increasing concentrations of Metformin and Rotenone. Results represent % growth rate \pm SD compared to non-treated controls (n=3). **b** Cell death of RPMI-8226 wild type (WT) (black) and bortezomib-resistant (BTZ/100) (grey) cells after a 48-hour treatment with increasing concentrations of phenformin or simvastatin. Results represent % cell death \pm SD (n=3). **c** LC-MS analysis of intracellular cholesterol (left panel) and CoQ (right panel) in RPMI-8226, AMO-1 and ARH-77 wild type (WT) (black) cells, bortezomib-resistant (dark grey) and carfilzomib resistant (light grey). Results represent relative peak area of metabolite \pm SD compared to WT cells (n=3). **d** Growth rate of RPMI-8226 wild type (WT) (black) and bortezomib-resistant (BTZ/100) (grey) cells after a 48-hour treatment with 1 μ M simvastatin, atorvastatin or rosuvastatin. Results represent % growth rate \pm SD compared to non-treated controls (n=3). **e** Cell viability of AMO-1 and ARH-77 wild type (WT) and bortezomib-resistant cells after a 48-hour treatment with 1 μ M Simvastatin. Results represent % cell viability \pm SD compared to non-treated controls (n=3). **f** LC-MS analysis of intracellular cholesterol (left panel) and CoQ (right panel) in RPMI-8226, AMO-1 and ARH-77 wild type (WT) (black) cells, bortezomib-resistant (dark grey) and carfilzomib resistant (light grey), cells after a 24-hour treatment with 1 μ M simvastatin. Results represent relative peak area of metabolite \pm SD compared to non-treated controls cells (n=3). **g** LC-MS analysis of intracellular cholesterol (left panel) and CoQ (right panel) in RPMI-8226 wild type (WT) (black) and bortezomib-resistant (BTZ/100) (grey) cells after a 24-hour treatment with 1 μ M simvastatin, atorvastatin or rosuvastatin. Results represent relative peak area of metabolite \pm SD compared to non-treated controls (n=3). **h** LC-MS analysis of extracellular lactate levels of WT (black) and BTZ/100 cells (grey) after 24 hours treatment with 1 μ M simvastatin. Data represents relative peak area of metabolite \pm SD compared to non-treated controls (n=3). **i** Cell viability of AMO-1 and ARH-77 wild type (WT) and bortezomib-resistant cells after a 48-hour treatment with bortezomib (ARH-77 WT: 1nM, AMO-1 WT: 2nM and BTZ-resistant 100 nM) with and without a 24-hour preincubation with 100 nM (AMO-1) or 30 nM (ARH-77) simvastatin. Results represent % cell viability \pm SD compared to non-treated controls (n=3). One-way ANOVA tests were performed (* = p<0.05, ** = p<0.01, *** = p<0.001, **** = p<0.0001)